



Degree Project in Medical Engineering
Second cycle, 30 credits

Real-Time Biomechanical Analysis of Human Movement with Wearable Sensors and Musculoskeletal Modelling

BERGÞÓRA HLÍN SIGURÐARDÓTTIR

Real-Time Biomechanical Analysis of Human Movement with Wearable Sensors and Musculoskeletal Modelling

Bergþóra Hlín Sigurðardóttir

Master's Programme, Medical Engineering, 120 Credits

Supervisor: Ruoli Wang

Reviewer: Mikael Forsman

Examiner: Matilda Larsson

School of Engineering Sciences in Chemistry, Biotechnology and Health

Swedish Title: Biomekanisk analys av mänskliga rörelser i realtid med bärbara sensorer och muskuloskeletala modeller

Abstract

Motion analysis is widely used in medicine, ergonomics, and sports science, but traditional motion capture (MoCap) systems are expensive and limited to laboratory settings. Wearable sensors offer a more accessible alternative for capturing movement in everyday life, but no existing system enables accurate, real-time estimation of joint kinematics and kinetics. This project aimed to validate a wearable sensor system that combines inertial measurement units (IMUs), pressure insoles, and musculoskeletal modelling for real-time estimation of hip, knee, and ankle joint angles and moments. Data were collected from three participants using the wearable system and a laboratory-based MoCap system, which served as a reference, during static, dynamic, and walking tasks. Real-time estimates from the wearable system were then compared to offline MoCap outputs. The results showed good overall agreement for joint angles and ankle moments, while larger errors were observed for hip and knee moments. While further validation is needed, the findings suggest that the system has potential for real-time biomechanical analysis outside the laboratory.

Keywords

Wearable sensors, real-time motion analysis, musculoskeletal modelling, inertial measurement units (IMUs), pressure insoles, joint kinematics and kinetics, biomechanics

Sammanfattning

Rörelseanalys används i stor utsträckning inom medicin, ergonomi och idrottsvetenskap, men traditionella rörelseanalyssystem (MoCap) är dyra och begränsade till laboratoriemiljöer. Bärbara sensorer erbjuder ett mer tillgängligt alternativ för att analysera rörelser i vardagen, men inget befintligt system möjliggör noggrann, realtidsuppskattning av ledkinematik och ledkinetik. Det här projektet syftade till att validera ett bärbart sensorsystem som kombinerar tröghetsmätningenheter (IMU:er), tryckinlägg och muskuloskeletal modellering för realtidsuppskattning av höft-, knä- och fotledsvinklar samt moment. Data samlades in från tre deltagare med hjälp av det bärbara systemet och ett laboriebaserat MoCap-system, som fungerade som referens, under statiska, dynamiska och gångrelaterade uppgifter. Realtidsuppskattningarna från det bärbara systemet jämfördes sedan med offlineresultat från MoCap. Resultaten visade god överensstämmelse för ledvinklar och fotledsmoment, medan större fel observerades för höft- och knämoment. Även om ytterligare validering behövs, tyder resultaten på att det bärbara systemet har potential för att användas för biomekanisk analys i realtid utanför laboratoriet.

Nyckelord

Bärbara sensorer, rörelseanalys i realtid, muskuloskeletal modellering, inertiellavmätinstrument (IMU), tryckmätande sulor, ledkinematik och ledkinetik, biomekanik

Acknowledgements

I want to thank my supervisor, Ruoli Wang, for her feedback and guidance throughout the project. I am especially grateful to Zhaoyuan Wan, PhD student at the KTH MoveAbility Lab, for his continuous support. His generous time, help, and patience were instrumental throughout the process. Thank you to Frederico Belmonte Klein for developing the wearable system.

Thank you to my group supervisor, Maksims Kornevs, for always being available to answer questions, provide feedback, and offer support. I also want to thank my reviewer, Mikael Forsman, for his thoughtful feedback on my report.

Finally, I would like to thank my family and friends back home for their unconditional support and encouragement. To my mom and dad, thank you for always supporting me. And to my Geir, thank you for always believing in me.

Abbreviations

2D two-dimensional

3D three-dimensional

CGM Conventional Gait Model

CoP center of pressure

EMG electromyography

GRF ground reaction force

ID inverse dynamics

IK inverse kinematics

IMU inertial measurement unit

MoCap motion capture

RMSE root mean square error

ROS Robot Operating System

SD standard deviation

SO static optimization

STS sit-to-stand and stand-to-sit

Contents

1	Introduction	2
1.1	Project Aim	3
1.2	Thesis Outline	3
2	Background	4
2.1	Motion Analysis	4
2.1.1	Kinematics and Kinetics	5
2.1.2	Biomechanical Models	5
2.2	Motion Capture Systems	6
2.3	Wearable Sensors	8
2.3.1	Inertial Measurement Units	8
2.3.2	Pressure Insoles	9
2.4	Recent Work	9
2.4.1	Integrated Wearable Sensor Systems	9
2.4.2	Real-Time Motion Analysis	10
3	Methodology	12
3.1	Equipment	12
3.1.1	Wearable Sensor System	12
3.1.2	Motion Capture System	13
3.2	Participants	14
3.2.1	Selection	14
3.2.2	Preparation	14
3.3	Data Collection	15
3.3.1	Static Tasks	15
3.3.2	Dynamic Tasks	15

3.3.3	Walking Tasks	16
3.4	Post-Processing of Motion Capture Data	16
3.5	Data Analysis	16
4	Results	18
4.1	Static Tasks	18
4.2	Dynamic Tasks	21
4.3	Walking Tasks	22
5	Discussion	26
5.1	Static Tasks	26
5.2	Dynamic Tasks	27
5.3	Walking Tasks	28
5.4	Limitations	28
5.5	Future Work	29
5.6	Social, Ethical, and Sustainability Aspects	29
6	Conclusions	30
	References	32
A	Additional Results	40
A.1	Static Tasks	40
A.2	Dynamic Tasks	41
A.3	Walking Tasks	43

List of Figures

2.1.1	The Gait2392 musculoskeletal model. Modified from [28].	6
2.2.1	Reconstructed 3D model from the Vicon system [29].	7
3.1.1	Simplified flowchart of the real-time data processing pipeline used in the wearable system.	13
3.2.1	Experimental setup showing the equipment used and sensor placement on participants. Components of the wearable system (IMUs and pressure insoles) are labelled in red, and MoCap system components are labelled in blue. Modified from [43].	14
4.1.1	Box plots comparing joint angles and moments during natural stance, estimated using the wearable and MoCap systems. Red lines indicate the median, blue boxes show the interquartile range, and black whiskers represent ± 1 SD. One participant was excluded due to IMU drift.	19
4.1.2	Box plots comparing joint angles and moments during single-leg stance, shown separately for the left side (a) and right side (b). Estimates from the wearable and MoCap systems are shown. Red lines indicate the median, blue boxes the interquartile range, and black whiskers ± 1 SD. One participant was excluded due to IMU drift.	20
4.2.1	Joint angles (top row) and moments (bottom row) during squat. The red line with dashed bounds shows the mean ± 1 SD from the wearable system. The blue line with the shaded area shows the mean ± 1 SD from the MoCap system.	21
4.2.2	Joint angles (top row) and moments (bottom row) during vertical jump. The red line with dashed bounds shows the mean ± 1 SD from the wearable system. The blue line with the shaded area shows the mean ± 1 SD from the MoCap system.	22

- 4.3.1 Joint angles (top row) and moments (bottom row) during normal walking. The red line with dashed bounds shows the mean ± 1 SD from the wearable system. The blue line with the shaded area shows the mean ± 1 SD from the MoCap system. 23
- 4.3.2 Joint angles (top row) and moments (bottom row) during fast walking. The red line with dashed bounds shows the mean ± 1 SD from the wearable system. The blue line with the shaded area shows the mean ± 1 SD from the MoCap system. 24

List of Tables

4.1.1	RMSE values for hip, knee, and ankle joint angles and moments during natural and single-leg stance. Left and right sides are reported separately for single-leg stance. Values are presented as mean ± 1 SD. One participant was excluded due to IMU drift.	19
4.2.1	RMSE values for hip, knee, and ankle joint angles and moments during squat and vertical jump. Values are presented as mean ± 1 SD.	22
4.3.1	RMSE values for hip, knee, and ankle joint angles and moments during normal and fast walking. Values are presented as mean ± 1 SD.	23

Chapter 1

Introduction

Motion analysis is widely used in medicine, ergonomics, and sports science, providing quantitative insights into the biomechanics of the musculoskeletal system during movement. It combines motion capture (MoCap) technologies with biomechanical modelling to estimate kinematic and kinetic parameters, such as joint angles and moments, that describe how the body moves and the forces involved. These parameters are essential for identifying abnormal movement patterns, supporting decision-making, and evaluating treatment outcomes [1], [2]. Traditional MoCap systems, consisting of cameras and force plates, are considered the gold standard for motion analysis due to their high accuracy [3]. However, these systems are expensive, require time-consuming setup, and are limited to controlled laboratory settings, making them less suitable for capturing natural movement in everyday environments [4].

Wearable sensors, including inertial measurement units (IMUs) and pressure insoles, have emerged as a promising alternative for studying human movement in real-world settings [5]. IMUs are compact devices integrating accelerometers, gyroscopes, and magnetometers to capture body segment kinematics [6]. They are affordable, easy to use, and have been applied in clinical and research contexts to detect gait abnormalities, assess fall risk, and capture joint angles during functional tasks [7], [8]. Pressure insoles are lightweight and unobtrusive sensors embedded in footwear to estimate kinetic variables such as ground reaction forces (GRFs) and center of pressure (CoP). They have minimal impact on natural movement, making them suitable for both static and dynamic assessments [9], [10], [11].

Recent studies have focused on integrating IMUs and pressure insoles into a single

wearable system to simultaneously capture kinematic and kinetic data, enabling more comprehensive motion analysis [12]. Manupibul et al. [13] validated such a system against a traditional MoCap setup and demonstrated strong agreement. However, the study was limited to one participant and one walking task. Wang et al. [12] extended this work with a larger sample and a broader range of movements, reporting strong agreement for joint angles and ankle moments, but reduced accuracy for hip and knee moments. While these studies showed promising results for estimating joint angles and moments, they relied on offline data processing, limiting their ability to provide real-time feedback.

Real-time motion analysis addresses this limitation by enabling direct interaction with biomechanical data as it is collected. Practitioners can visualise key variables immediately, enhancing performance feedback and clinical decision-making. Real-time systems have been developed using musculoskeletal modelling tools, such as OpenSimRT, which can estimate joint angles and moments in real time [14], [15]. However, no existing system combines both IMUs and pressure insoles for real-time estimation of joint kinematics and kinetics. This gap highlights the need for an integrated wearable sensor system that enables accurate, real-time biomechanical analysis of human movement outside the laboratory.

1.1 Project Aim

This project aimed to validate a wearable sensor system that combines IMUs, pressure insoles, and musculoskeletal modelling for real-time estimation of hip, knee, and ankle joint angles and moments. The outputs generated by the wearable system were compared with those obtained from a laboratory-based MoCap system across a range of static, dynamic, and walking tasks.

1.2 Thesis Outline

This thesis is structured as follows. Chapter 2 introduces the theoretical background, including motion analysis, MoCap systems, wearable sensors, and recent work on integrated and real-time systems. Chapter 3 describes the methodology, Chapter 4 presents the results, followed by Chapter 5, which discusses the findings, limitations, and future directions. Finally, Chapter 6 concludes the thesis.

Chapter 2

Background

This chapter outlines key concepts relevant to this project, including motion analysis, kinematics and kinetics, biomechanical modelling, traditional MoCap systems, and their limitations. It also covers wearable sensors, particularly IMUs and pressure insoles, and recent work on integrated wearable systems and real-time analysis.

2.1 Motion Analysis

Human movement is a complex, coordinated process involving bones, muscles, ligaments, and joints of the musculoskeletal system and is regulated by the nervous system. The musculoskeletal system generates forces and joint moments that allow the body to maintain stability and perform controlled movements under varying conditions. When any component of this system is impaired, movement can become unstable, inefficient, or restricted [1].

To understand how such impairments affect movement, motion analysis offers quantitative insight into the biomechanics of the musculoskeletal system. It is widely applied in medicine, ergonomics, and sports science, combining MoCap technologies with biomechanical modelling to capture the three-dimensional (3D) movements of body segments and measure external forces acting on the body. These data are then used to estimate kinematic and kinetic parameters, such as joint angles and moments, that describe how the body moves and the forces involved. These parameters are essential for identifying abnormal movement patterns, guiding clinical decision-making, and assessing treatment outcomes [1], [2], [16].

The key variables derived from motion analysis are typically categorised into kinematics and kinetics, which are estimated using biomechanical models that mathematically represent the human body [1]. The following sections provide a detailed overview of these concepts.

2.1.1 Kinematics and Kinetics

Kinematics describes the movement of body segments, specifically how their position and orientation change over time. It defines motion geometrically using displacement, velocity, and acceleration without considering the forces that produce it. Kinematic data is typically collected using MoCap systems, which track the 3D positions of markers placed on the body. These trajectories are then used to estimate joint angles through a process known as inverse kinematics (IK) [17].

In contrast, kinetics focuses on the forces and moments that drive movement [18]. Movement results from the interaction of internal and external forces [1]. Skeletal muscles generate internal forces that create joint moments and produce movement [19]. GRFs act on the body during contact with the ground, and the CoP represents the point under the foot where these forces are applied [20]. Joint forces and moments can be estimated using inverse dynamics (ID), which combines kinetic data, such as GRFs and CoP, with kinematic measurements [1].

2.1.2 Biomechanical Models

Biomechanical models are widely used in motion analysis to simulate human movement. They represent the musculoskeletal system mathematically, allowing for non-invasive analysis of the body's mechanical behaviour. These models vary in complexity and are developed using different computational approaches [21]. One of the most commonly used models in clinical gait analysis is the Conventional Gait Model (CGM) [22]. It is based on a rigid body modelling approach, where the body is represented as a series of rigid segments connected by joints [23]. The CGM is implemented in the Vicon MoCap system and is used to estimate joint kinematics and kinetics [24].

Musculoskeletal models provide a more detailed mechanical representation of the body. In these models, bones are modelled as rigid segments connected by joints,

while muscles are defined according to their anatomical structure and force-generating properties. Musculoskeletal models estimate internal forces, such as muscle and joint reaction forces, based on measured movement and external loads [25]. They are often implemented in simulation platforms such as OpenSim, a widely used tool for modelling, simulating, and analysing the musculoskeletal system. OpenSim integrates kinematic and kinetic data from MoCap systems and includes tools for scaling generic models to match individual anthropometry. It also supports IK for calculating joint angles, ID for computing joint moments, and static optimization (SO) for estimating individual muscle forces and activations [26]. A commonly used musculoskeletal model in OpenSim is the Gait2392 model, which provides a comprehensive representation of the lower limbs and torso [27]. A schematic of this model is shown in Figure 2.1.1.

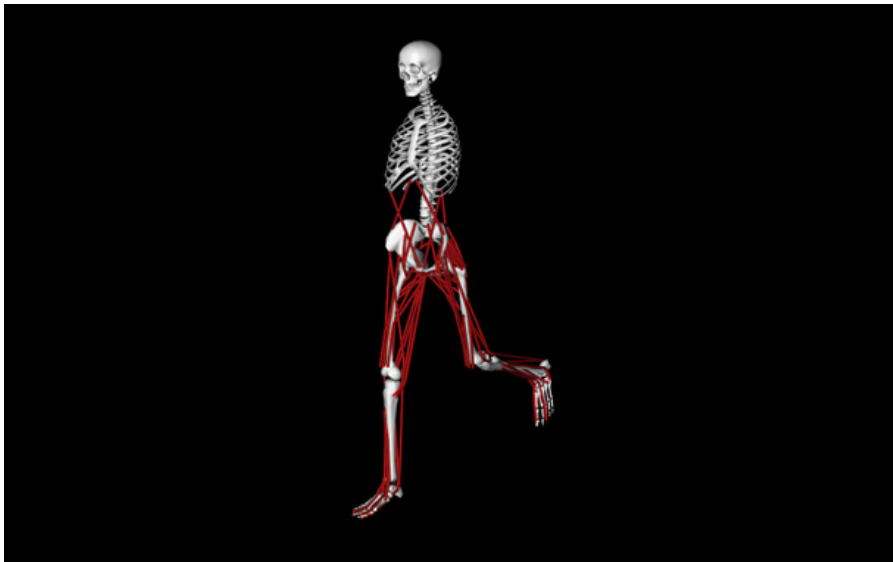


Figure 2.1.1: The Gait2392 musculoskeletal model. Modified from [28].

2.2 Motion Capture Systems

MoCap systems are widely considered the gold standard for motion analysis due to their high accuracy in capturing kinematic and kinetic data [3]. These systems typically consist of optical cameras, force plates, instrumented treadmills, and surface electromyography (EMG), enabling a comprehensive analysis of human movement [29]. One of the most commonly used MoCap systems is Vicon, which employs multiple infrared cameras to track reflective markers placed on anatomical landmarks [30]. Each camera captures two-dimensional (2D) images from different angles, which

are then combined to estimate the 3D positions of the markers, allowing for precise tracking of body motion over time [29]. A visual example of a reconstructed 3D model from a Vicon system is shown in Figure 2.2.1.

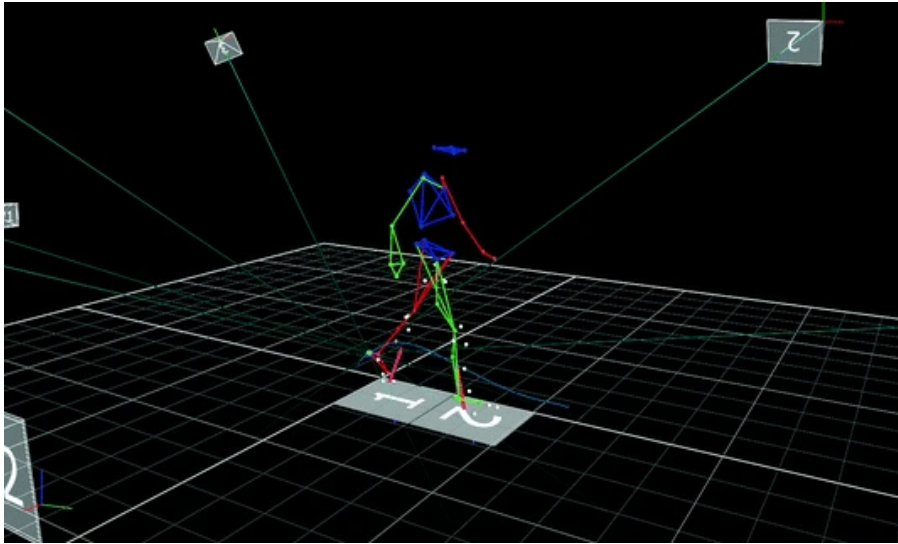


Figure 2.2.1: Reconstructed 3D model from the Vicon system [29].

In addition to optical tracking, other components are used to capture external forces and muscle activity. Force plates are mechanical sensors that measure GRFs and the CoP during human movement. They detect forces through slight deformation of embedded sensors, which generate voltage signals proportional to the applied load [31]. Force plates are typically embedded in the ground or integrated into treadmills [32]. When embedded in a treadmill, they provide continuous measurements of kinetic data during walking or running [33]. To assess muscle activity, EMG is used to measure the electrical signals generated during movement, providing insight into activation patterns and each muscle's contribution to human motion [1], [32].

Despite their precision, MoCap systems have several limitations. The setup is time-consuming and requires trained personnel to ensure consistent and accurate marker placement. Marker positioning can vary between sessions or clinicians, which affects data quality, and markers may interfere with natural movement or be influenced by soft tissue artefacts [34]. These systems are also expensive, restricted to controlled laboratory environments, and require extensive post-processing. They are less accessible for patients in remote areas or with limited mobility and are not well suited for capturing natural movement in everyday settings [4], [9].

2.3 Wearable Sensors

To address the limitations of traditional MoCap systems, wearable sensors have emerged as a promising alternative for studying human movement in real-world settings [5]. These sensors are not confined to controlled environments, making them suitable for continuous monitoring in daily life [35]. IMUs and pressure insoles are the most commonly used wearable sensors for capturing kinematic and kinetic data [12].

2.3.1 Inertial Measurement Units

IMUs are compact, wearable devices that integrate accelerometers, gyroscopes, and often magnetometers to capture the kinematics of body segments during movement. Accelerometers measure linear and gravitational acceleration, providing information on segment motion and orientation. Gyroscopes measure angular velocity, capturing the rotational movement of the body segment where the IMU is attached. Magnetometers estimate orientation by detecting the Earth's magnetic field, similar to a compass. The data from these sensors is transmitted wirelessly to an external device, where algorithms process and combine signals from multiple IMUs to estimate kinematic parameters [6].

IMUs enable motion tracking without the constraints of traditional MoCap systems, making them well-suited for collecting biomechanical data in real-world environments. They are increasingly used in clinical and research settings due to their portability, affordability, and ease of use [7]. In clinical settings, IMUs have been used to detect gait abnormalities, assess fall risk, and monitor disease progression in patients with conditions like stroke, Parkinson's disease, and osteoarthritis [8]. They have also been applied to balance assessment and fall detection in remote settings [35]. IMUs can effectively distinguish between healthy and impaired gait patterns and have been shown to accurately capture joint kinematics during dynamic movements, such as squats and lunges [36], [37].

Despite these advantages, IMUs have several limitations. They are susceptible to integration drift, which can reduce accuracy over time. Magnetometers can be affected by nearby magnetic interference, and incorrect sensor placement may result in inaccurate data [7].

2.3.2 Pressure Insoles

Pressure insoles are wearable devices integrating pressure sensors into footwear to measure the interaction between the foot and the ground during movement [8]. These sensors convert mechanical pressure into electrical signals, allowing for the estimation of GRFs, CoP, and pressure distribution across the foot [38]. Unlike laboratory-based force plates, pressure insoles offer a portable and practical solution for collecting movement data in real-world settings, with greater flexibility and ease of use [10].

These sensors are lightweight, unobtrusive, and have minimal impact on natural movement, making them suitable for long-term monitoring [9]. Pressure insoles have been used to monitor gait patterns and balance in clinical populations and have been shown to accurately capture GRFs and CoP during walking, running, and other functional tasks [10], [11], [39].

However, pressure insoles have some limitations. Mechanical wear over time can affect performance, and environmental factors like humidity and temperature inside the shoe may cause signal drift and reduce accuracy [8].

2.4 Recent Work

The following sections outline recent work on integrated wearable sensor systems and real-time motion analysis.

2.4.1 Integrated Wearable Sensor Systems

Recent studies have focused on combining IMUs and pressure insoles into a single wearable system to simultaneously capture kinematic and kinetic data, enabling more comprehensive motion analysis outside the laboratory [12]. Manupibul et al. [13] developed such a system and compared joint angles and moments with those obtained from a traditional MoCap setup. The results showed strong agreement, but the study was limited to one participant and a single walking condition.

Wang et al. [12] extended this work using nine participants and 13 movement tasks, including walking, running, squats, lunges, and vertical jumps. The system showed strong agreement for lower limb joint angles, vertical GRFs, and ankle moments, moderate agreement for anterior-posterior CoP and knee moments, but

poor agreement for hip moments and mediolateral CoP.

While these studies show promising results for estimating joint kinematics and kinetics using integrated wearable systems, they rely on offline data processing. Traditionally, motion analysis is performed after data collection, with motion and force data processed offline to estimate biomechanical variables such as joint angles and moments. Although this approach provides valuable insights, it does not allow for real-time feedback [14].

2.4.2 Real-Time Motion Analysis

In contrast to offline processing, real-time motion analysis allows for direct interaction with movement data as it is collected. These systems enable practitioners to visualise and quantify biomechanical variables in real time. Presenting this information during movement can provide immediate feedback, potentially improving performance beyond what is possible with verbal or tactile instruction alone [14].

Van den Bogert et al. [14] developed a real-time system based on a musculoskeletal model capable of estimating joint angles, moments, and muscle forces using IK, ID, and SO. However, the model was generic and did not incorporate subject-specific anatomical features, limiting its use for personalised assessments.

Pizzolato et al. [15] introduced a real-time OpenSim-based framework that estimated joint angles and moments using data from a traditional MoCap system. The system used subject-scaled musculoskeletal models, and the real-time results closely matched those from offline OpenSim analyses. Similarly, Stanev et al. [40] developed a real-time system to estimate joint angles and moments using both MoCap and IMU-based data, with strong agreement between real-time and offline results.

Despite advances in wearable sensor technology and real-time analysis, no existing system combines both IMUs and pressure insoles for real-time estimation of joint kinematics and kinetics [12]. This gap highlights the need for a system integrating wearable sensors with musculoskeletal modelling, enabling accurate, real-time biomechanical analysis of human movement outside the laboratory.

Chapter 3

Methodology

This chapter describes the methodology for validating a wearable sensor system for real-time estimation of hip, knee, and ankle joint angles and moments. The system was evaluated by comparing its outputs with those from a laboratory-based MoCap system across a range of static, dynamic, and walking tasks. The chapter outlines the experimental equipment, participant selection and preparation, data collection, post-processing, and analysis procedures.

3.1 Equipment

This section describes the equipment used for data collection, including the wearable sensor system and the laboratory-based MoCap system used as a reference.

3.1.1 Wearable Sensor System

The wearable sensor system used in this project was previously developed at the MoveAbility Lab at KTH. It consisted of eight IMUs (x-IMU3, x-io Technologies, UK) and a pair of pressure insoles (OpenGo version 3, Moticon, Germany), both collecting data at 100 Hz. Data from the sensors was processed in real time using the Robot Operating System (ROS), which was structured into three processing nodes: IK, ID, and SO.

The IK node estimated joint angles from the orientation data provided by the IMUs, each measuring the 3D orientation of its corresponding body segment. These data were

passed to OpenSimRT, a real-time musculoskeletal modelling platform based on the Gait2392 model [40]. Joint angles were calculated from the relative orientations of adjacent segments and then used as input to the ID and SO nodes.

Vertical GRFs and CoP positions were measured using the pressure insoles. These signals were synchronized and transformed to align with the IMU data in both time and reference frames. The ID node used the joint angles and external forces to compute joint moments. The SO node estimated muscle activations by solving for muscle force distributions that reproduced the joint moments while minimizing total effort. The output indicated the activation level of each muscle as a percentage of its maximum force. Figure 3.1.1 shows a simplified flowchart of the real-time processing pipeline used in the wearable system.

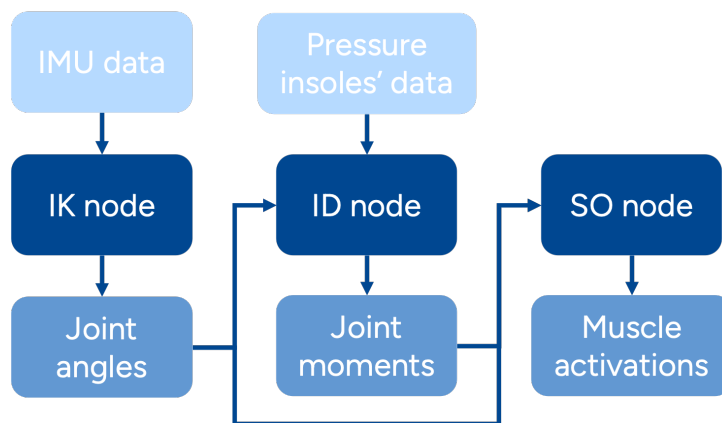


Figure 3.1.1: Simplified flowchart of the real-time data processing pipeline used in the wearable system.

3.1.2 Motion Capture System

The MoCap system included infrared cameras, force plates, an instrumented treadmill, and EMG sensors. Marker trajectories were captured using ten cameras (VICON Vantage V16, Vicon, UK) operating at 100 Hz. GRFs were measured at 1000 Hz using four force plates (AMTI Optima, AMTI, USA) and an instrumented treadmill (AMTI Tandem, AMTI, USA). Muscle activity was recorded using six EMG sensors (Pico EMG, Cometa, Italy), placed on each leg, also operating at 1000 Hz. Marker, GRF, and EMG data were recorded simultaneously.

3.2 Participants

This section outlines the participant selection criteria and preparation procedures before data collection.

3.2.1 Selection

Three participants (age: 28.3 ± 1.3 years, height: 1.73 ± 0.08 m, weight: 63.1 ± 9.8 kg; two male, one female), with no known history of neurological or musculoskeletal impairments, were recruited for the study. Participants were required to wear EU shoe sizes 38, 39, 42, or 43 to match the available pressure insole sizes. Ethical approval from each participant was obtained prior to data collection.

3.2.2 Preparation

Anthropometric measurements were collected to scale the musculoskeletal models in Vicon and OpenSimRT. Participants wore standardised footwear fitted with pressure insoles. EMG sensors were placed on six lower limb muscles on each leg, following SENIAM guidelines [41]. Reflective markers were positioned according to the CGM 2.3 marker set [42], with two additional markers placed on the pelvis for post-processing. IMUs were placed on the trunk, pelvis, thighs, shanks, and feet using custom holders. The complete experimental setup is shown in Figure 3.2.1.

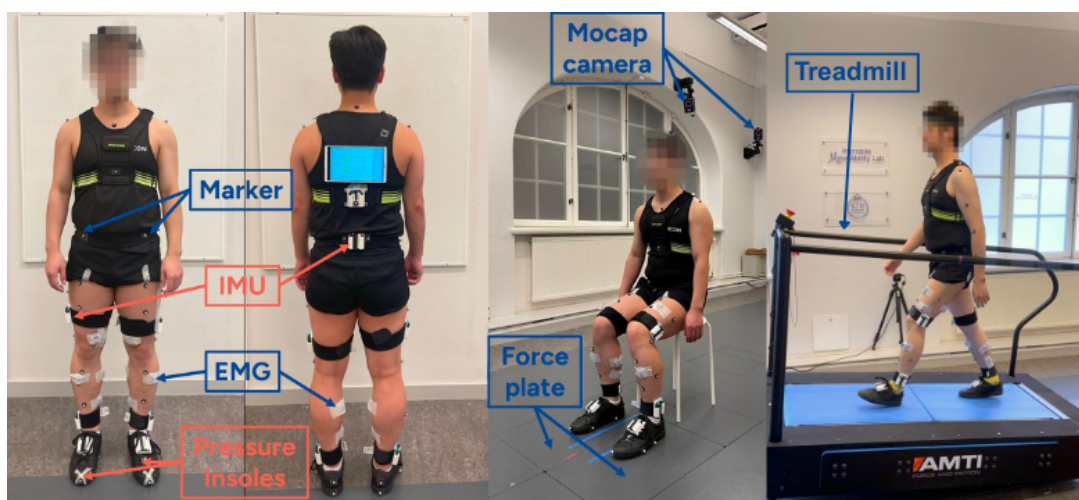


Figure 3.2.1: Experimental setup showing the equipment used and sensor placement on participants. Components of the wearable system (IMUs and pressure insoles) are labelled in red, and MoCap system components are labelled in blue. Modified from [43].

3.3 Data Collection

Data were collected simultaneously from the wearable system and the MoCap system at the KTH MoveAbility Lab. Each participant completed a series of tasks, grouped into three categories: static, dynamic, and walking. Two trials were recorded per task for each participant.

3.3.1 Static Tasks

Participants performed four static postures on flat ground, each held for 30 seconds. For tasks involving both feet on the ground, each foot was placed on a separate force plate:

1. Natural stance: Feet shoulder-width apart in a relaxed posture.
2. Narrow stance: Feet as close together as possible without touching.
3. Single-leg stance: Standing on the dominant leg with the other leg lifted, knee bent, and shin parallel to the ground.
4. Tandem stance: Heel-to-toe position with the dominant foot placed in front.

3.3.2 Dynamic Tasks

Participants completed four dynamic tasks on flat ground:

1. Lunge: Five forward lunges with the dominant leg, lowering the body until the front knee aligned with the ankle and the back knee was close to the ground, then returning to standing.
2. Squat: Five bodyweight squats with feet shoulder-width apart, lowering until the thighs were roughly parallel to the ground, then returning to standing.
3. Sit-to-stand and stand-to-sit (STS): Five repetitions rising from a seated position to standing and back down, performed with arms crossed over the torso.
4. Vertical jump: Three jumps from standing, starting with a squat and jumping upward.

3.3.3 Walking Tasks

Participants performed five walking tasks on an instrumented treadmill. Each trial lasted 20 seconds:

1. Normal walking: Self-selected comfortable speed.
2. Slow walking: Fixed speed of 0.5 m/s.
3. Fast walking: Fixed speed of 1.0 m/s.
4. Incline walking: Self-selected speed on a 10% incline.
5. Decline walking: Self-selected speed on a 10% decline.

3.4 Post-Processing of Motion Capture Data

MoCap data were processed in Vicon Nexus (version 2.16; Vicon Motion Systems Ltd., Oxford, UK) using a standard post-processing pipeline [44]. Each trial was segmented manually by visually inspecting the data and marking the start and end points of each task.

For static tasks, a 10-second segment from the middle of each trial was marked. For dynamic tasks, the start and end points of each repetition were defined as follows: lunges from toe-off to return to standing, squats from the start of knee flexion to full extension, STS from seat-off to recontact with the stool, and vertical jumps from the start of the downward motion to landing. For walking tasks, gait cycles were identified based on heel strikes detected by the treadmill force plates.

3.5 Data Analysis

Data analysis was performed in MATLAB (version R2022a; The MathWorks Inc., Natick, MA, USA), focusing on sagittal plane joint angles and moments at the hip, knee, and ankle. Joint moments were normalised to body weight. One trial per task was selected for analysis for each participant. The data segments identified during post-processing were used to extract corresponding MoCap and wearable data for comparison.

A time offset correction was applied to enable accurate comparison between systems. For dynamic and walking tasks, the first prominent peak in the knee joint angle trajectory was identified in both systems, and the time offset was calculated and applied to the wearable data. For static tasks, where no clear peaks were present, the median offset from the dynamic and walking tasks was used instead.

For static tasks, average joint angles and moments were calculated for each participant from the 10-second segment. These values were then averaged across participants to generate box plots and compute root mean square error (RMSE) values to assess agreement between the two systems. Data from the natural and narrow stance tasks were analysed with the left and right sides combined. For the single-leg stance, sides were analysed separately, as all participants used the same dominant foot.

For dynamic tasks, three movement cycles were extracted from each trial. Squats, STS, and vertical jumps were analysed with sides combined, while lunges were analysed per side, since all participants performed them with the same dominant leg. For walking tasks, five gait cycles were extracted from each trial and analysed with sides combined. All cycles were time-normalised to a 0–100% scale, then averaged per participant and across participants to generate joint angle and moment curves and compute RMSE values.

Chapter 4

Results

This chapter presents joint angle and moment results for the hip, knee, and ankle, estimated using the wearable sensor system and the MoCap system. Results are reported across static, dynamic, and walking tasks. Tandem stance was excluded due to data quality issues, and decline walking was excluded due to gait cycle detection errors during post-processing.

The results focus on selected tasks to demonstrate the performance of the wearable system across different types of movement. These include natural stance, single-leg stance, squat, vertical jump, normal walking, and fast walking. Results for the remaining tasks, including narrow stance, lunge, STS, slow walking, and incline walking, are provided in Appendix A.

For static tasks, results are shown as box plots of average joint angles and moments, calculated from 10-second segments for each participant and averaged across participants. For dynamic and walking tasks, joint angles and moments are presented as time-normalized curves, averaged over multiple movement cycles per participant and across participants. For each task, the agreement between the two systems was assessed using RMSE.

4.1 Static Tasks

This section presents results for the natural stance and single-leg stance tasks. Due to IMU drift, data from only two participants were included. Figures 4.1.1 and 4.1.2 show

box plots of joint angles and moments from both systems.

In the natural stance, the largest differences were observed at the hip and knee angles, which is reflected in the higher RMSE values in Table 4.1.1. In the single-leg stance, discrepancies were most noticeable at the hip on the left (lifted) side, while knee and ankle angles were more closely aligned. On the right (stance) side, knee moment errors were higher, also indicated by the RMSE values. Across both tasks, joint moment differences remained relatively small.

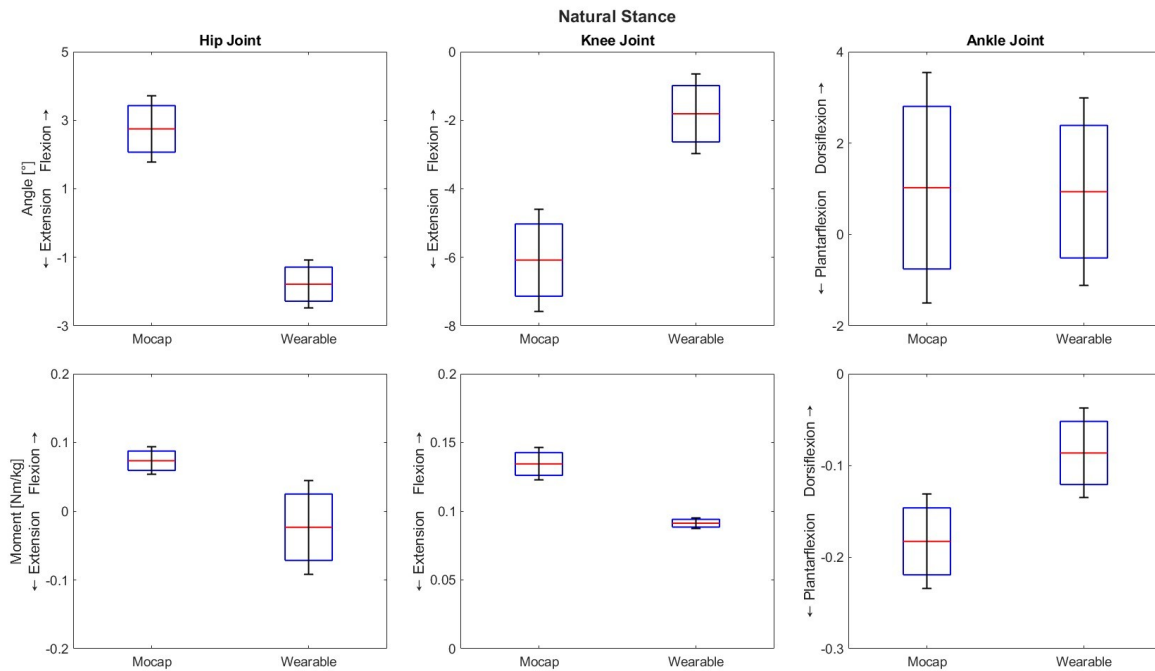
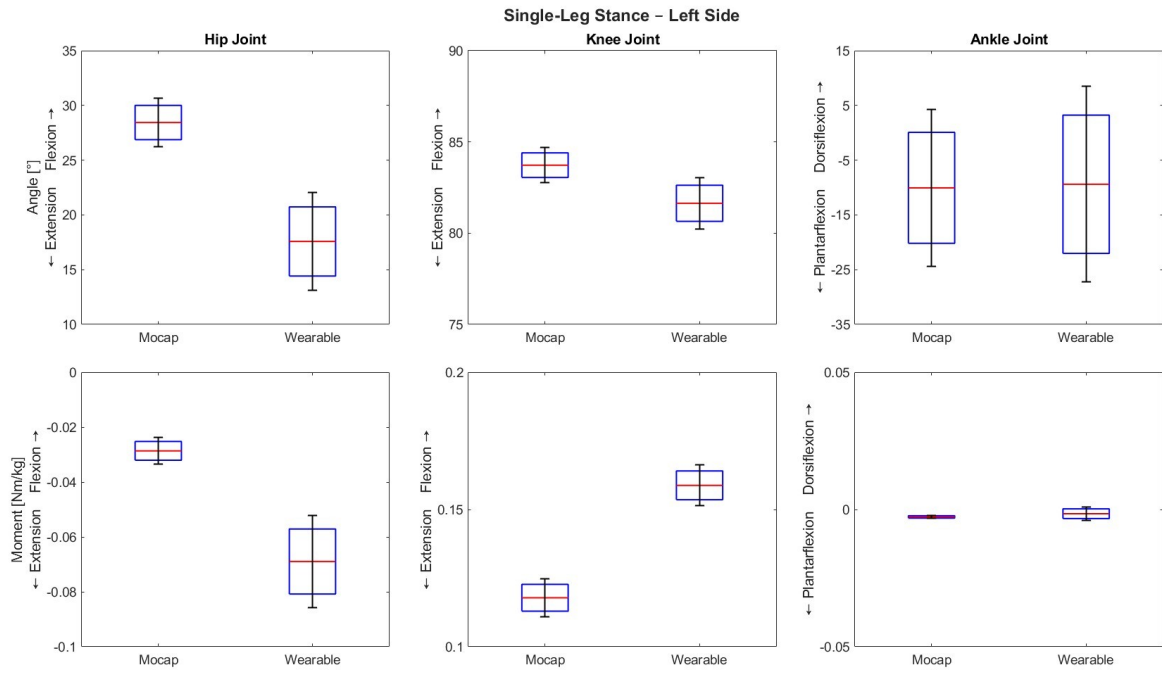


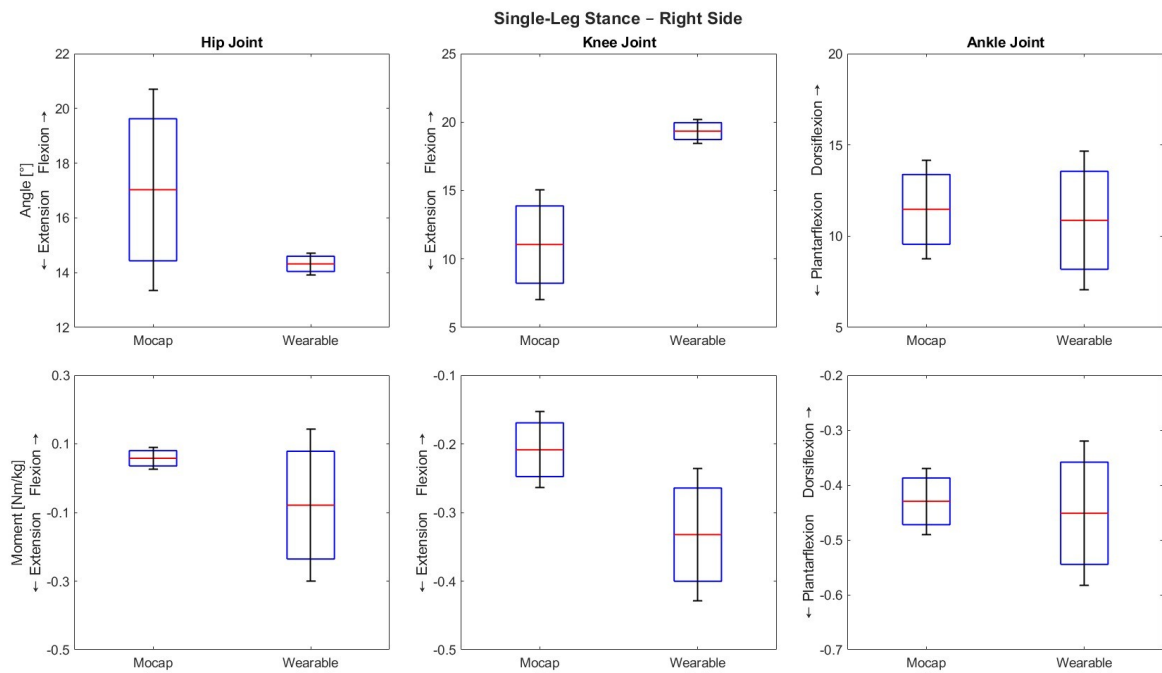
Figure 4.1.1: Box plots comparing joint angles and moments during natural stance, estimated using the wearable and MoCap systems. Red lines indicate the median, blue boxes show the interquartile range and black whiskers represent ± 1 standard deviation (SD). One participant was excluded due to IMU drift.

Table 4.1.1: RMSE values for hip, knee, and ankle joint angles and moments during natural and single-leg stance. Left and right sides are reported separately for single-leg stance. Values are presented as mean ± 1 SD. One participant was excluded due to IMU drift.

Variable	Joint	Natural	Single-leg	
			Left side	Right side
Angle [°]	Hip	4.53 \pm 1.66	10.86 \pm 6.68	2.71 \pm 3.28
	Knee	4.27 \pm 2.65	2.09 \pm 0.44	8.29 \pm 4.87
	Ankle	0.33 \pm 0.12	2.49 \pm 0.93	0.77 \pm 0.85
Moment [Nm/kg]	Hip	0.10 \pm 0.05	0.04 \pm 0.02	0.14 \pm 0.19
	Knee	0.04 \pm 0.02	0.04 \pm 0.01	0.12 \pm 0.04
	Ankle	0.10 \pm 0.00	0.00 \pm 0.00	0.05 \pm 0.03



(a) Left (lifted) side.



(b) Right (stance) side.

Figure 4.1.2: Box plots comparing joint angles and moments during single-leg stance, shown separately for the left side (a) and right side (b). Estimates from the wearable and MoCap systems are shown. Red lines indicate the median, blue boxes the interquartile range, and black whiskers ± 1 SD. One participant was excluded due to IMU drift.

4.2 Dynamic Tasks

This section presents results for the squat and vertical jump tasks. Figures 4.2.1 and 4.2.2 show sagittal plane joint angles and moments from both systems. The angle curves followed similar overall patterns, but the wearable system tended to underestimate joint angles at peak flexion, particularly during the squat task. As shown in Table 4.2.1, the largest RMSE occurred at the hip during squats and at the knee during vertical jumps.

For joint moments, estimates at the hip and knee during squats were similar between systems, while the wearable system consistently overestimated ankle moments. In the vertical jump, larger discrepancies were observed at the hip and knee, while ankle moments showed better agreement. Across both tasks, the hip had the highest RMSE, while the lowest errors were at the knee in the squat and at the ankle in the vertical jump.

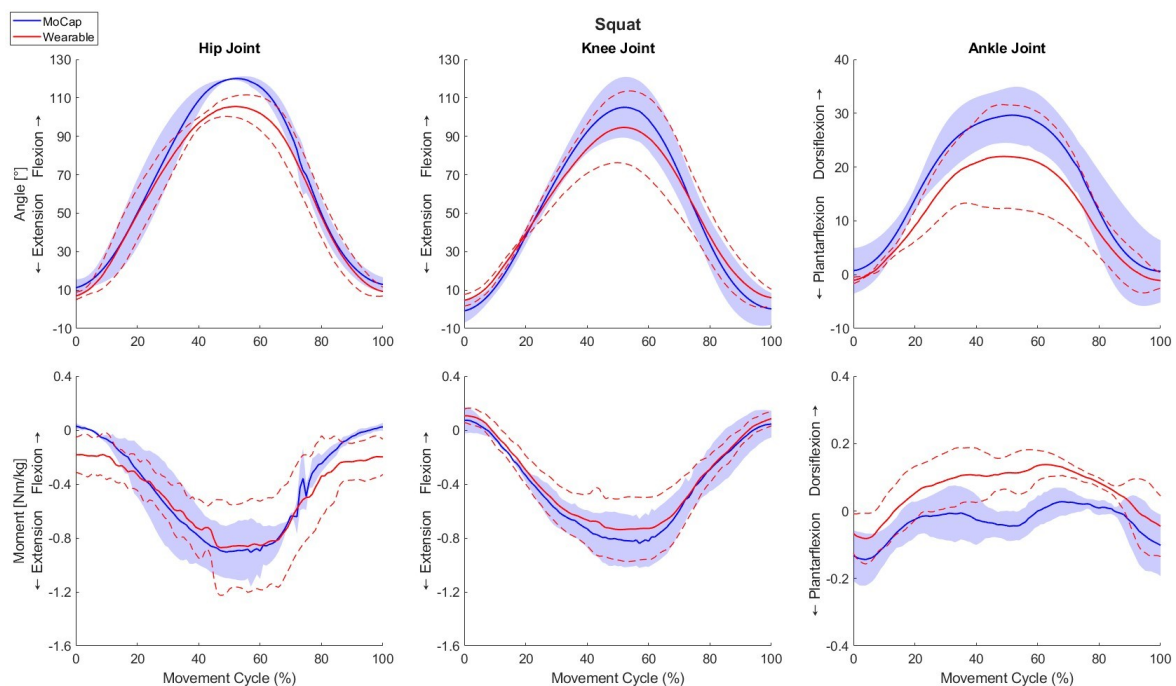


Figure 4.2.1: Joint angles (top row) and moments (bottom row) during squat. The red line with dashed bounds shows the mean ± 1 SD from the wearable system. The blue line with the shaded area shows the mean ± 1 SD from the MoCap system.

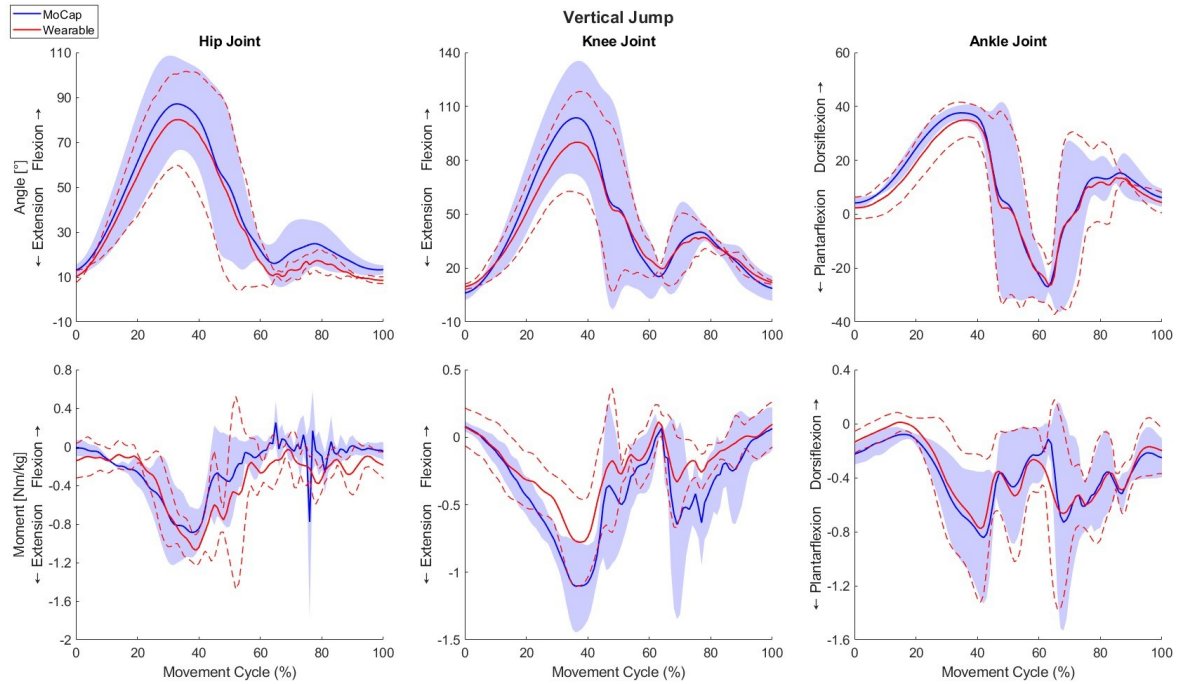


Figure 4.2.2: Joint angles (top row) and moments (bottom row) during vertical jump. The red line with dashed bounds shows the mean ± 1 SD from the wearable system. The blue line with the shaded area shows the mean ± 1 SD from the MoCap system.

Table 4.2.1: RMSE values for hip, knee, and ankle joint angles and moments during squat and vertical jump. Values are presented as mean ± 1 SD.

Variable	Joint	Squat	Vertical Jump
Angle [°]	Hip	8.45 ± 3.57	6.71 ± 4.91
	Knee	7.03 ± 3.98	7.82 ± 2.48
	Ankle	6.10 ± 6.19	5.10 ± 3.67
Moment [Nm/kg]	Hip	0.24 ± 0.14	0.29 ± 0.07
	Knee	0.08 ± 0.07	0.23 ± 0.03
	Ankle	0.10 ± 0.04	0.12 ± 0.06

4.3 Walking Tasks

This section presents results for the normal and fast walking tasks. Figures 4.3.1 and 4.3.2 show sagittal plane joint angles and moments from both systems. The angle curves followed similar patterns overall, but the wearable system consistently underestimated hip angles. As shown in Table 4.3.1, the largest angle RMSE occurred at the hip, while the smallest was at the ankle in both walking tasks.

For joint moments, ankle estimates closely matched those from the MoCap system, whereas larger differences were observed at the hip and knee. This pattern is reflected

in the RMSE values, with the highest errors at the hip and the lowest at the ankle. Although the joint angle and moment curves were generally similar between walking tasks across all joints, the wearable system showed greater differences during fast walking, which is also reflected in the higher RMSE values.

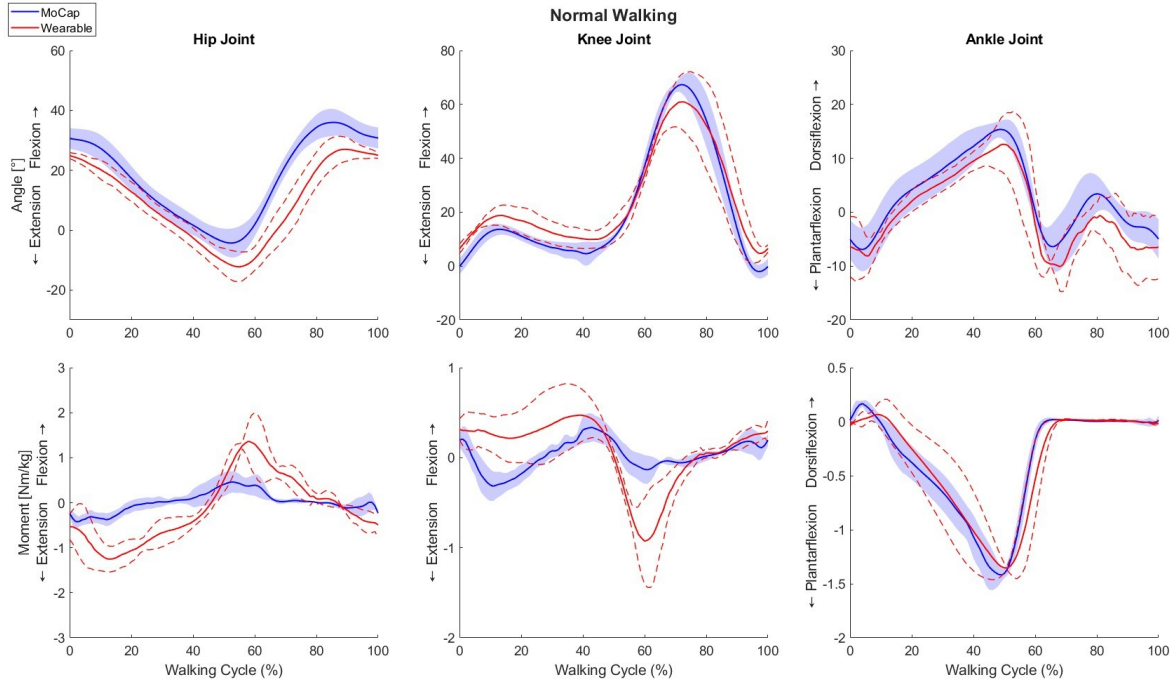


Figure 4.3.1: Joint angles (top row) and moments (bottom row) during normal walking. The red line with dashed bounds shows the mean ± 1 SD from the wearable system. The blue line with the shaded area shows the mean ± 1 SD from the MoCap system.

Table 4.3.1: RMSE values for hip, knee, and ankle joint angles and moments during normal and fast walking. Values are presented as mean ± 1 SD.

Variable	Joint	Normal	Fast
Angle [°]	Hip	9.53 ± 0.93	13.59 ± 4.95
	Knee	7.12 ± 1.01	6.46 ± 2.45
	Ankle	3.85 ± 3.53	5.04 ± 3.03
Moment [Nm/kg]	Hip	0.65 ± 0.18	0.76 ± 0.19
	Knee	0.40 ± 0.09	0.47 ± 0.13
	Ankle	0.15 ± 0.06	0.12 ± 0.04

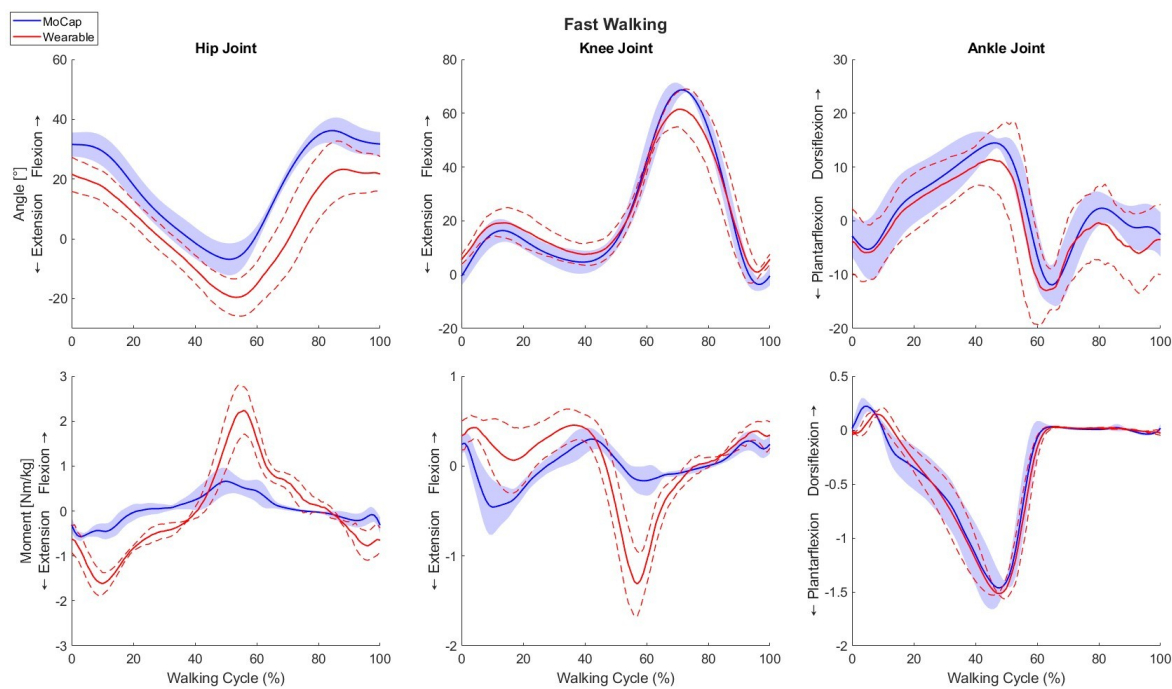


Figure 4.3.2: Joint angles (top row) and moments (bottom row) during fast walking. The red line with dashed bounds shows the mean ± 1 SD from the wearable system. The blue line with the shaded area shows the mean ± 1 SD from the MoCap system.

Chapter 5

Discussion

This study aimed to validate a wearable sensor system for real-time estimation of hip, knee, and ankle joint angles and joint moments by comparing its outputs to those from a MoCap system across a range of static, dynamic, and walking tasks. This chapter discusses the main findings and limitations, and outlines directions for future work to improve and extend the system. It also reflects on the social, ethical, and sustainability aspects of the wearable system.

The SO node was included in the wearable system; however, its output consistently showed a recurring one-second gap across all trials and participants, resulting in missing data throughout each recording. Because the results were generated in real time, these gaps could not be recovered or corrected, and muscle activation estimates were excluded from the final analysis. Additionally, a time delay was observed between the wearable and MoCap systems, which may have affected the comparisons and contributed to higher RMSE values. While a correction algorithm was developed, it was not robust enough to fully account for the delay in all cases. This delay likely influenced agreement between systems, but it does not affect the estimations from the wearable system itself, as it is not intended to be used alongside MoCap setups in the future.

5.1 Static Tasks

For static tasks, the agreement between the wearable system and the MoCap system was generally good, based on visual inspection and the computed RMSE values.

However, the results are based on only two participants, as data from a third had to be excluded due to noticeable IMU drift. During data collection, the OpenSimRT model was monitored in real time to ensure it was tracking the participant's movement correctly. In some cases, the tracking was inaccurate, indicating that the IMUs had drifted and needed recalibration before the subsequent trial. This drift was sometimes not noticed until later during data analysis, which led to a few trials being excluded from the final analysis.

With data from only two participants, statistical analysis could not be conducted to determine whether the observed differences were significant, which limits the generalisability of the findings. Some variation was also seen across joints, with higher errors possibly caused by small postural shifts affecting IMU orientation. These errors were especially relevant in tasks requiring participants to remain still, where even subtle movements could introduce noticeable inaccuracies.

5.2 Dynamic Tasks

For dynamic tasks, the wearable system captured the overall patterns of joint angles and moments during both squats and vertical jumps. In squats, joint angles were generally underestimated at peak flexion, possibly due to IMU strap movement. Increased pelvic and hip motion may have also contributed to the higher errors observed at the hip. In vertical jumps, the largest angle errors occurred at the knee, likely due to the greater range and speed of motion at the knee joint. Rapid flexion and extension may have introduced soft tissue artefacts or caused slight sensor misalignment, which could have reduced the accuracy of the joint angle estimates.

Across both tasks, the ankle showed the smallest errors, while the hip showed the largest. These results are consistent with findings from Wang et al. [12], who reported increased angle errors with greater joint motion, particularly at the hip and knee, during dynamic movements. Joint moment errors followed a similar pattern, with higher errors at the hip and smaller errors at the ankle. The moment errors may be explained by inaccuracies in joint angle estimates and limitations in CoP estimations, both of which likely contributed to reduced accuracy in moment calculations.

5.3 Walking Tasks

The wearable system produced joint angle patterns generally consistent with the MoCap system during normal and fast walking tasks. Knee and ankle angle RMSE values were similar to those reported in previous studies [45], [46], while errors at the hip were noticeably higher. One possible explanation is the difference in reference frame definitions between systems. The MoCap system accounts for anterior pelvic tilt in the standing position, whereas the wearable system does not, which results in lower hip angle estimates. Angle errors increased during fast walking, likely due to higher movement speed and greater soft tissue artefacts. Similar trends have been reported in earlier work, where faster walking and running were associated with higher errors [12], [47].

Compared to joint angles, joint moments showed greater deviations at the hip and knee in both walking tasks, while ankle moments were more closely aligned between systems. RMSE values followed a similar pattern, with the highest moment errors at the hip and the lowest at the ankle. The absence of horizontal GRFs from the pressure insoles likely contributed to the larger moment errors at the hip and knee. These proximal joints are more affected by missing horizontal forces due to their longer moment arms, making them more sensitive to incomplete force data than distal joints like the ankle [12]. Joint angle errors may have also contributed to the inaccuracies in moment estimates.

5.4 Limitations

Several limitations affected the results of the study. One was the small number of participants. Although three participants were recruited, some results were based on only two due to data quality issues. With such a small sample size, it is difficult to assess the consistency of the system's performance across individuals or to draw conclusions that can be generalised to a broader population.

Another limitation was that the pressure insoles used in the wearable system measured only the vertical component of the GRFs. The absence of horizontal forces likely reduced the accuracy of joint moment estimates at the hip and knee, especially during walking, where horizontal forces are more pronounced. Although some studies have explored methods to estimate horizontal forces [48], [49], achieving reliable estimates

across a range of movements remains challenging.

5.5 Future Work

While this project provides an initial step in validating an integrated wearable system for real-time motion analysis, several areas should be addressed in future work. A key next step is to evaluate the performance of the SO node by comparing its real-time outputs to offline results to ensure it functions as intended. Once resolved, muscle activation estimates could be included in future validation studies. Collecting data from more participants is also important to assess how consistent the results are across individuals and to improve the generalisability of the findings.

Another area for improvement is addressing the time delay between systems. A more robust approach could improve signal alignment across recordings and increase the overall accuracy of system comparisons. Finally, future work should explore ways to improve joint moment estimates at the hip and knee, particularly by addressing the absence of horizontal GRF measurements in the current setup.

5.6 Social, Ethical, and Sustainability Aspects

The wearable system used in this project has the potential to make motion analysis more accessible in clinical and rehabilitation settings where laboratory-based equipment is not available. Real-time monitoring outside the laboratory could support earlier detection of movement issues, track recovery, and provide more personalised feedback in home-based rehabilitation. While wearable systems may reduce reliance on large laboratory setups, the environmental impact of sensor production, use, and disposal should be considered in future development. All participants gave informed consent, and no identifiable personal data were stored or used. Data were handled responsibly throughout the project.

Chapter 6

Conclusions

This project aimed to validate an integrated wearable sensor system that combines IMUs, pressure insoles, and musculoskeletal modelling for real-time estimation of hip, knee, and ankle joint angles and moments across static, dynamic, and walking tasks. Data were collected from three participants, using the same wearable system and a laboratory-based MoCap system simultaneously. Real-time outputs from the wearable system were compared to offline MoCap results, which were used as a reference.

The system showed good overall agreement for joint angles and ankle moments, while larger errors were observed for hip and knee moments. Future work should focus on evaluating the performance of the SO node to enable reliable muscle activation estimates, addressing the absence of horizontal GRF measurements in the current setup, and validating the system with a larger sample size.

To conclude, the system successfully provided real-time estimates of hip, knee, and ankle joint angles and moments across various movement tasks and shows strong potential for real-time motion analysis outside the laboratory.

References

- [1] T.-W. Lu and C.-F. Chang, “Biomechanics of human movement and its clinical applications,” *The Kaohsiung Journal of Medical Sciences*, vol. 28, no. 2 Suppl, S13–S25, Feb. 2012. DOI: 10.1016/j.kjms.2011.08.004.
- [2] A. Horwood and N. Chockalingam, “Introduction,” in *Clinical Biomechanics in Human Locomotion: Gait and Pathomechanical Principles*, Academic Press, 2023, pp. xxiii–xxv. [Online]. Available: <https://doi.org/10.1016/B978-0-443-15860-5.09983-9>.
- [3] N. Zahradka, K. Verma, A. Behboodi, B. Bodt, H. Wright, and S. C. K. Lee, “An Evaluation of Three Kinematic Methods for Gait Event Detection Compared to the Kinetic-Based ‘Gold Standard’,” *Sensors (Basel, Switzerland)*, vol. 20, no. 18, p. 5272, Sep. 2020. DOI: 10.3390/s20185272.
- [4] P. Huang, A. Mostovov, R. Cohen, C. Cadilhac, and R. Pionnier, “Comparison of feetme insoles with a motion capture system coupled to force plates for assessing gait and posture,” *Scientific Reports*, vol. 15, no. 1, p. 13 476, Apr. 2025. DOI: 10.1038/s41598-025-96878-8.
- [5] G. R. H. Regterschot, G. M. Ribbers, and Johannes B. J. Bussmann, “Wearable Movement Sensors for Rehabilitation: From Technology to Clinical Practice,” *Sensors*, vol. 21, no. 14, p. 4744, Jul. 2021. DOI: 10.3390/s21144744.
- [6] J. Ghattas and D. N. Jarvis, “Validity of inertial measurement units for tracking human motion: A systematic review,” *Sports Biomechanics*, vol. 23, no. 11, pp. 1853–1866, Nov. 2024. DOI: 10.1080/14763141.2021.1990383.
- [7] C. Gu, W. Lin, X. He, L. Zhang, and M. Zhang, “IMU-based motion capture system for rehabilitation applications: A systematic review,” *Biomimetic Intelligence and Robotics*, vol. 3, no. 2, p. 100 097, Jun. 2023. DOI: 10.1016/j.birob.2023.100097.

- [8] F. Porciuncula *et al.*, “Wearable Movement Sensors for Rehabilitation: A Focused Review of Technological and Clinical Advances,” *PM & R : the journal of injury, function, and rehabilitation*, vol. 10, no. 9 Suppl 2, S220–S232, 2018. DOI: 10.1016/j.pmrj.2018.06.013.
- [9] B. Oubre, S. Lane, S. Holmes, K. Boyer, and S. I. Lee, “Estimating Ground Reaction Force and Center of Pressure using Low-Cost Wearable Devices,” *IEEE transactions on bio-medical engineering*, vol. 69, no. 4, pp. 1461–1468, Apr. 2022. DOI: 10.1109/TBME.2021.3120346.
- [10] T. Cudejko, K. Button, and M. Al-Amri, “Wireless pressure insoles for measuring ground reaction forces and trajectories of the centre of pressure during functional activities,” *Scientific Reports*, vol. 13, p. 14 946, Sep. 2023. DOI: 10.1038/s41598-023-41622-3.
- [11] A. Pergolini *et al.*, “Assessment of Sensorized Insoles in Balance and Gait in Individuals With Parkinson’s Disease,” *IEEE Transactions on Neural Systems and Rehabilitation Engineering*, vol. 32, pp. 1445–1454, 2024. DOI: 10.1109/TNSRE.2024.3381537.
- [12] H. Wang, A. Basu, G. Durandau, and M. Sartori, “A wearable real-time kinetic measurement sensor setup for human locomotion,” *Wearable Technologies*, vol. 4, e11, Apr. 2023. DOI: 10.1017/wtc.2023.7.
- [13] U. Manupibul, R. Tanthuwapathom, W. Jarumethitanont, P. Kaimuk, W. Limroongreungrat, and W. Charoensuk, “Integration of force and IMU sensors for developing low-cost portable gait measurement system in lower extremities,” *Scientific Reports*, vol. 13, no. 1, p. 10 653, Jun. 2023. DOI: 10.1038/s41598-023-37761-2.
- [14] A. J. van den Bogert, T. Geijtenbeek, O. Even-Zohar, F. Steenbrink, and E. C. Hardin, “A real time system for biomechanical analysis of human movement and muscle function,” *Medical & Biological Engineering & Computing*, vol. 51, no. 10, pp. 1069–1077, Oct. 2013. DOI: 10.1007/s11517-013-1076-z.
- [15] C. Pizzolato, M. Reggiani, L. Modenese, and D. G. Lloyd, “Real time inverse kinematics and inverse dynamics for lower limb applications using OpenSim,” *Computer Methods in Biomechanics and Biomedical Engineering*, vol. 20, no. 4, pp. 436–445, Mar. 2017. DOI: 10.1080/10255842.2016.1240789.

- [16] S. J. Piazza, "Motion Analysis," in *Encyclopedia of Neuroscience*, M. D. Binder, N. Hirokawa, and U. Windhorst, Eds., Berlin, Heidelberg: Springer, 2009, pp. 2406–2409. [Online]. Available: https://doi.org/10.1007/978-3-540-29678-2_3567.
- [17] Y. Z. Arslan, D. Karabulut, F. Ortes, and M. B. Popovic, "11 - Exoskeletons, Exomusculatures, Exosuits: Dynamic Modeling and Simulation," in *Biomechatronics*, M. B. Popovic, Ed., Academic Press, 2019, pp. 305–331. [Online]. Available: <https://doi.org/10.1016/B978-0-12-812939-5.00011-2>.
- [18] A. S. Arockia Doss, P. K. Lingampally, G. M. T. Nguyen, and D. Schilberg, "A comprehensive review of wearable assistive robotic devices used for head and neck rehabilitation," *Results in Engineering*, vol. 19, p. 101306, Sep. 2023. DOI: 10.1016/j.rineng.2023.101306.
- [19] M. W. Whittle, "Chapter 1 - Basic sciences," in *Gait Analysis (Fourth Edition)*, M. W. Whittle, Ed., Edinburgh: Butterworth-Heinemann, 2007, pp. 1–45. [Online]. Available: <https://doi.org/10.1016/B978-075068883-3.50006-4>.
- [20] J. Richards, A. Chohan, and R. Erande, "Chapter 15 - Biomechanics," in *Tidy's Physiotherapy (Fifteenth Edition)*, S. B. Porter, Ed., Churchill Livingstone, 2013, pp. 331–368. [Online]. Available: <https://doi.org/10.1016/B978-0-7020-4344-4.00015-8>.
- [21] I. Roupa, M. R. da Silva, F. Marques, S. B. Gonçalves, P. Flores, and M. T. da Silva, "On the Modeling of Biomechanical Systems for Human Movement Analysis: A Narrative Review," *Archives of Computational Methods in Engineering*, vol. 29, pp. 4915–4958, May 2022. DOI: 10.1007/s11831-022-09757-0.
- [22] F. Leboeuf, R. Baker, A. Barré, J. Reay, R. Jones, and M. Sangeux, "The conventional gait model, an open-source implementation that reproduces the past but prepares for the future," *Gait & Posture*, vol. 69, pp. 235–241, Mar. 2019. DOI: 10.1016/j.gaitpost.2019.04.015.
- [23] R. Baker, F. Leboeuf, J. Reay, and M. Sangeux, "The Conventional Gait Model - Success and Limitations," in *Handbook of Human Motion*, Cham: Springer International Publishing, 2018, pp. 489–508. [Online]. Available: https://doi.org/10.1007/978-3-319-14418-4_25.

- [24] H. Kainz and M. H. Schwartz, “The importance of a consistent workflow to estimate muscle-tendon lengths based on joint angles from the conventional gait model,” *Gait & Posture*, vol. 88, pp. 1–9, Jul. 2021. DOI: 10.1016/j.gaitpost.2021.04.039.
- [25] M. S. Andersen, “4 - Introduction to musculoskeletal modelling,” in *Computational Modelling of Biomechanics and Biotribology in the Musculoskeletal System (Second Edition)*, ser. Woodhead Publishing Series in Biomaterials, Z. Jin, J. Li, and Z. Chen, Eds., Woodhead Publishing, 2021, pp. 41–80. [Online]. Available: <https://doi.org/10.1016/B978-0-12-819531-4.00004-3>.
- [26] A. Seth, M. Sherman, J. A. Reinbolt, and S. L. Delp, “OpenSim: A musculoskeletal modeling and simulation framework for in silico investigations and exchange,” *Procedia IUTAM*, vol. 2, pp. 212–232, 2011. DOI: 10.1016/j.piutam.2011.04.021.
- [27] H.-S. Lee, J.-H. Lee, and H.-S. Kim, “Activities of ankle muscles during gait analyzed by simulation using the human musculoskeletal model,” *Journal of Exercise Rehabilitation*, vol. 15, no. 2, pp. 229–234, Apr. 2019. DOI: 10.12965/jer.1938054.027.
- [28] Florian Michaud, “Neuromusculoskeletal human multibody models for the gait of healthy and spinal-cord-injured subjects,” en, Phd. Thesis, Universidade da Coruña, 2020. [Online]. Available: https://www.researchgate.net/publication/338854892_Neuromusculoskeletal_human_multibody_models_for_the_gait_of_healthy_and_spinal-cord-injured_subjects (visited on 03/09/2025).
- [29] A. Ancillao, “Stereophotogrammetry in Functional Evaluation: History and Modern Protocols,” in *Modern Functional Evaluation Methods for Muscle Strength and Gait Analysis*, A. Ancillao, Ed., Cham: Springer International Publishing, 2018, pp. 1–29. [Online]. Available: https://doi.org/10.1007/978-3-319-67437-7_1.
- [30] F. Roggio *et al.*, “Technological advancements in the analysis of human motion and posture management through digital devices,” *World Journal of Orthopedics*, vol. 12, no. 7, pp. 467–484, Jul. 2021. DOI: 10.5312/wjo.v12.i7.467.

- [31] K. A. Lamkin-Kennard and M. B. Popovic, “4 - Sensors: Natural and Synthetic Sensors,” in *Biomechatronics*, M. B. Popovic, Ed., Academic Press, 2019, pp. 81–107. [Online]. Available: <https://doi.org/10.1016/B978-0-12-812939-5.00004-5>.
- [32] G. A. Lichtwark, R. W. Schuster, L. A. Kelly, S. G. Trost, and A. Bialkowski, “Markerless motion capture provides accurate predictions of ground reaction forces across a range of movement tasks,” *Journal of Biomechanics*, vol. 166, p. 112 051, Mar. 2024. DOI: 10.1016/j.jbiomech.2024.112051.
- [33] A. Belli, P. Bui, A. Berger, A. Geysant, and J.-R. Lacour, “A treadmill ergometer for three-dimensional ground reaction forces measurement during walking,” *Journal of Biomechanics*, vol. 34, no. 1, pp. 105–112, Jan. 2001. DOI: 10.1016/S0021-9290(00)00125-1.
- [34] K. Das, T. de Paula Oliveira, and J. Newell, “Comparison of markerless and marker-based motion capture systems using 95% functional limits of agreement in a linear mixed-effects modelling framework,” *Scientific Reports*, vol. 13, p. 22 880, Dec. 2023. DOI: 10.1038/s41598-023-49360-2.
- [35] M. Giebler, J. Werth, B. Waltersberger, and K. Karamanidis, “A wearable sensor and framework for accurate remote monitoring of human motion,” *Communications Engineering*, vol. 3, pp. 1–15, Jan. 2024. DOI: 10.1038/s44172-024-00168-6.
- [36] N. A. Edwards, J. B. Caccese, R. E. Tracy, J. Hagen, C. C. Quatman-Yates, and J. OñATE, “The Validity and Usability of Markerless Motion Capture and Inertial Measurement Units for Quantifying Dynamic Movements,” *Medicine and science in sports and exercise*, vol. 57, no. 3, pp. 641–655, Mar. 2025. DOI: 10.1249/MSS.0000000000003579.
- [37] T. Sun *et al.*, “Inertial Sensor-Based Motion Analysis of Lower Limbs for Rehabilitation Treatments,” *Journal of Healthcare Engineering*, vol. 2017, 2017. DOI: 10.1155/2017/1949170.
- [38] V. M. Santos, B. B. Gomes, M. A. Neto, and A. M. Amaro, “A Systematic Review of Insole Sensor Technology: Recent Studies and Future Directions,” *Applied Sciences*, vol. 14, no. 14, p. 6085, Jul. 2024. DOI: 10.3390/app14146085.

- [39] L. A. Cramer, M. A. Wimmer, P. Malloy, J. A. O’Keefe, C. B. Knowlton, and C. Ferrigno, “Validity and Reliability of the Insole3 Instrumented Shoe Insole for Ground Reaction Force Measurement during Walking and Running,” *Sensors (Basel, Switzerland)*, vol. 22, no. 6, p. 2203, Mar. 2022. DOI: 10.3390/s22062203.
- [40] D. Stanev *et al.*, “Real Time Musculoskeletal Kinematics and Dynamics Analysis Using Marker- and IMU-Based Solutions in Rehabilitation,” *Sensors (Basel, Switzerland)*, vol. 21, no. 5, p. 1804, Mar. 2021. DOI: 10.3390/s21051804.
- [41] H. J. Hermens, B. Freriks, C. Disselhorst-Klug, and G. Rau, “Development of recommendations for SEMG sensors and sensor placement procedures,” *Journal of Electromyography and Kinesiology*, vol. 10, no. 5, pp. 361–374, Oct. 2000. DOI: 10.1016/S1050-6411(00)00027-4.
- [42] Pycgm2, *CGM 2.3*. [Online]. Available: <https://pycgm2.netlify.app/cgm/cgm2.3/> (visited on 03/24/2025).
- [43] Z. Wan, F. B. Klein, H. Wang, and R. Wang, “A real-time full-chain biomechanical analysis framework based on integrated wearable sensors and musculoskeletal simulation,” Presented at 20th International Symposium on Computer Simulation in Biomechanics, not published in proceedings, Uppsala, Sweden, Jul. 2025.
- [44] *Vicon Nexus User Guide - Nexus 2.16 documentation - Vicon Help*. [Online]. Available: <https://help.vicon.com/space/Nexus216/11605325/Vicon+Nexus+User+Guide> (visited on 05/10/2025).
- [45] M. Al Borno *et al.*, “OpenSense: An open-source toolbox for inertial-measurement-unit-based measurement of lower extremity kinematics over long durations,” *Journal of NeuroEngineering and Rehabilitation*, vol. 19, no. 1, p. 22, Feb. 2022. DOI: 10.1186/s12984-022-01001-x.
- [46] T. McGrath and L. Stirling, “Body-Worn IMU-Based Human Hip and Knee Kinematics Estimation during Treadmill Walking,” *Sensors*, vol. 22, no. 7, p. 2544, Mar. 2022. DOI: 10.3390/s22072544.
- [47] C. Nüesch, E. Roos, G. Pagenstert, and A. Mündermann, “Measuring joint kinematics of treadmill walking and running: Comparison between an inertial sensor based system and a camera-based system,” *Journal of Biomechanics*, vol. 57, pp. 32–38, May 2017. DOI: 10.1016/j.jbiomech.2017.03.015.

REFERENCES

- [48] M. Hajizadeh, A. L. Clouthier, M. Kendall, and R. B. Graham, “Predicting vertical and shear ground reaction forces during walking and jogging using wearable plantar pressure insoles,” *Gait & Posture*, vol. 104, pp. 90–96, Jul. 2023. DOI: 10.1016/j.gaitpost.2023.06.006.
- [49] H. H. C. M. Savelberg and A. L. H. d. Lange, “Assessment of the horizontal, fore-aft component of the ground reaction force from insole pressure patterns by using artificial neural networks,” *Clinical Biomechanics*, vol. 14, no. 8, pp. 585–592, Oct. 1999. DOI: 10.1016/S0268-0033(99)00036-4.

Appendix A

Additional Results

A.1 Static Tasks

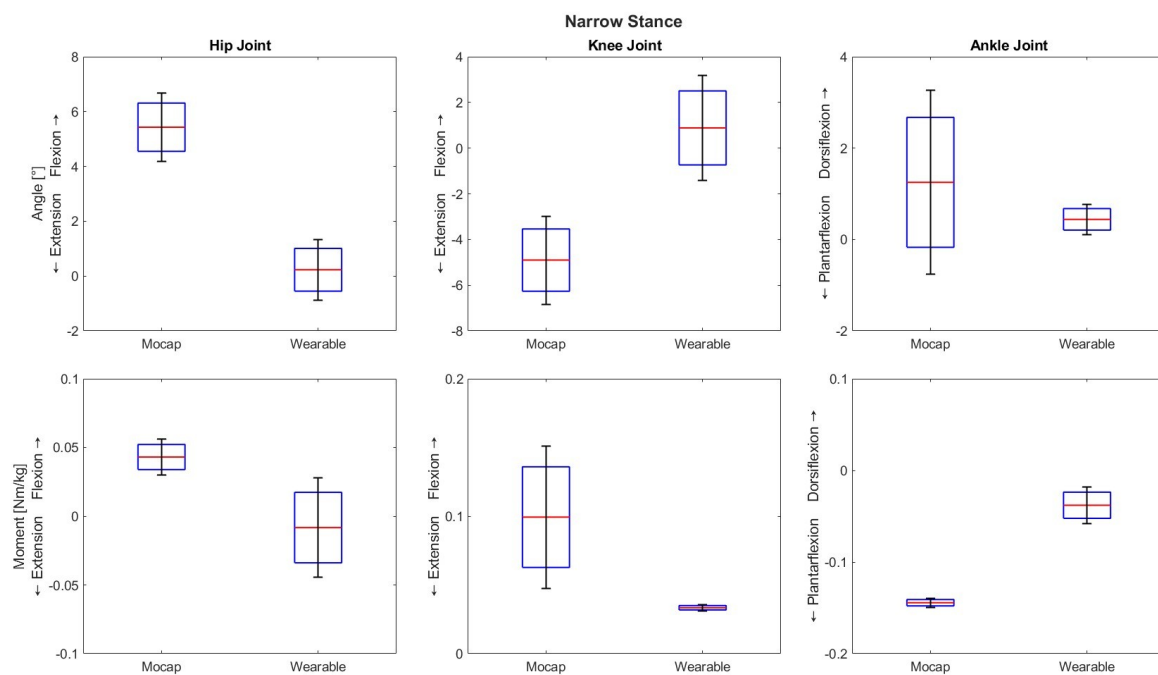


Figure A.1.1: Box plots comparing joint angles and moments during narrow stance, estimated using the wearable and MoCap systems. Red lines indicate the median, blue boxes show the interquartile range and black whiskers represent ± 1 SD. One participant was excluded due to IMU drift.

Table A.1.1: RMSE values for hip, knee, and ankle joint angles and moments during narrow stance. Values are presented as mean ± 1 SD. One participant was excluded due to IMU drift.

Variable	Joint	Narrow
Angle [°]	Hip	5.20 \pm 0.14
	Knee	5.79 \pm 0.36
	Ankle	1.19 \pm 1.15
Moment [Nm/kg]	Hip	0.05 \pm 0.05
	Knee	0.07 \pm 0.05
	Ankle	0.11 \pm 0.02

A.2 Dynamic Tasks

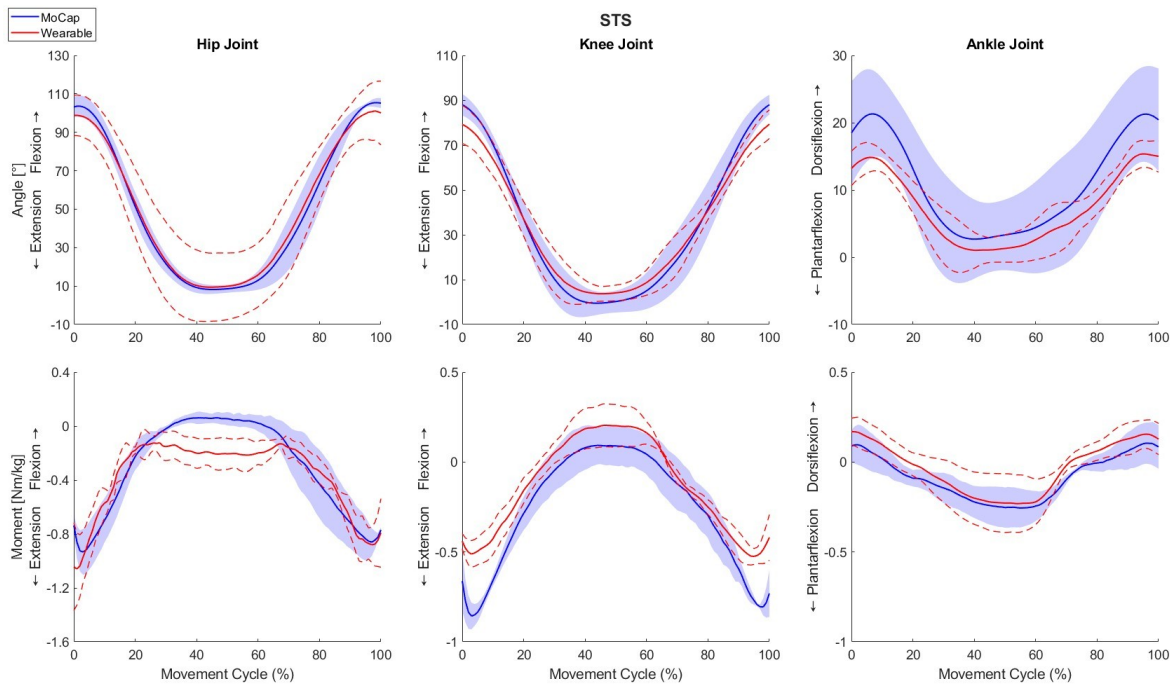


Figure A.2.1: Joint angles (top row) and moments (bottom row) during STS. The red line with dashed bounds shows the mean ± 1 SD from the wearable system. The blue line with the shaded area shows the mean ± 1 SD from the MoCap system.

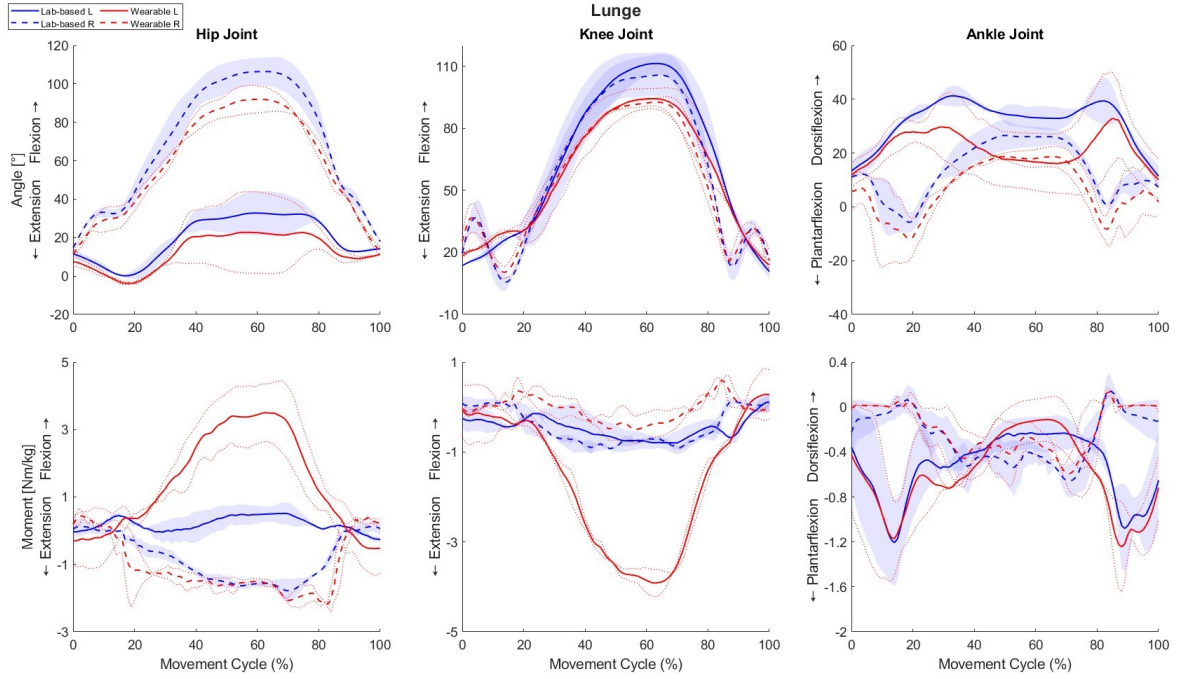


Figure A.2.2: Joint angles (top row) and moments (bottom row) during lunge, shown separately for the left side and right side. The red lines with dashed bounds show the mean ± 1 SD from the wearable system. The blue lines with the shaded area show the mean ± 1 SD from the MoCap system. One participant was excluded due to IMU drift.

Table A.2.1: RMSE values for hip, knee, and ankle joint angles and moments during STS and lunge. For lunge, left and right sides are reported separately, and one participant was excluded due to IMU drift. Values are presented as mean ± 1 SD.

Variable	Joint	STS	Lunge	
			Left side	Right side
Angle [°]	Hip	11.67 ± 6.44	7.46 ± 5.66	11.93 ± 6.92
	Knee	6.23 ± 1.79	10.37 ± 1.47	9.34 ± 3.98
	Ankle	4.49 ± 4.02	12.47 ± 9.66	7.22 ± 5.88
Moment [Nm/kg]	Hip	0.19 ± 0.05	1.82 ± 0.32	0.51 ± 0.07
	Knee	0.18 ± 0.10	1.75 ± 0.20	0.52 ± 0.05
	Ankle	0.07 ± 0.02	0.15 ± 0.03	0.11 ± 0.03

A.3 Walking Tasks

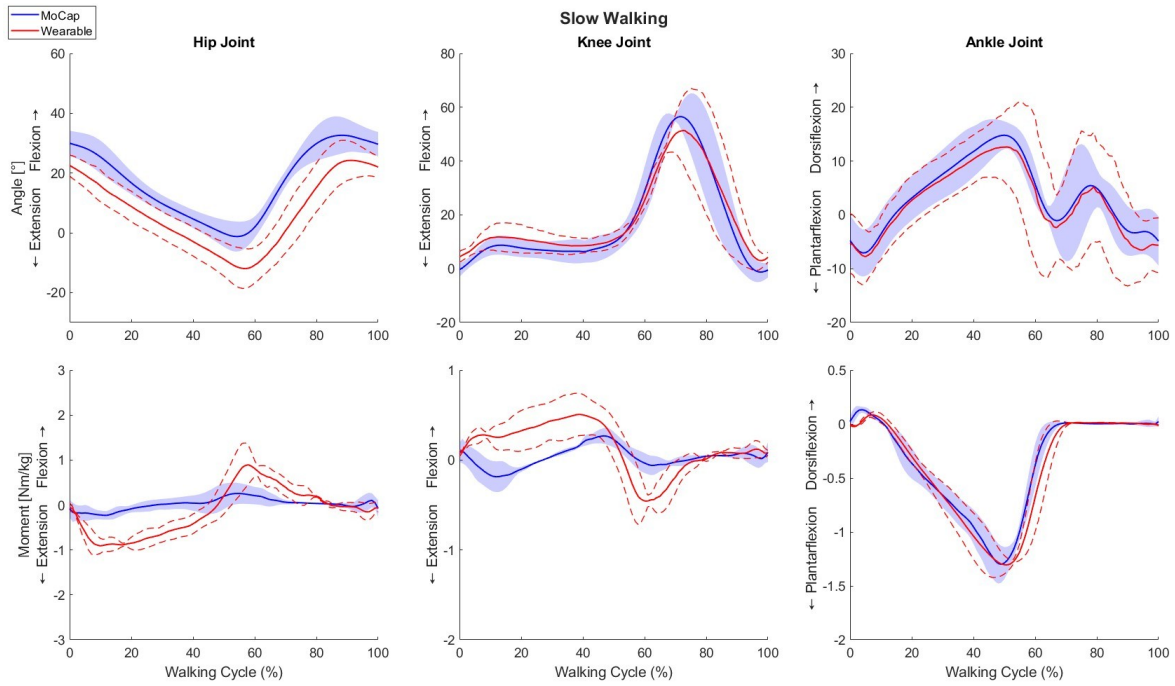


Figure A.3.1: Joint angles (top row) and moments (bottom row) during slow walking. The red line with dashed bounds shows the mean ± 1 SD from the wearable system. The blue line with the shaded area shows the mean ± 1 SD from the MoCap system.

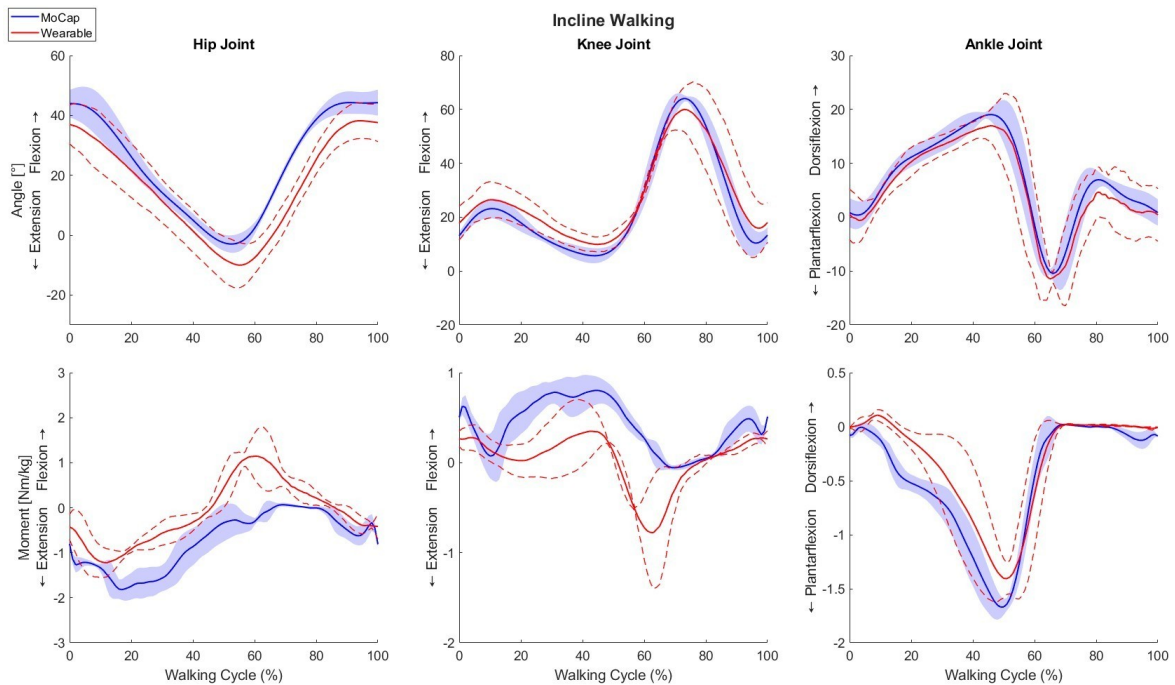


Figure A.3.2: Joint angles (top row) and moments (bottom row) during incline walking. The red line with dashed bounds shows the mean ± 1 SD from the wearable system. The blue line with the shaded area shows the mean ± 1 SD from the MoCap system.

Table A.3.1: RMSE values for hip, knee, and ankle joint angles and moments during slow and incline walking. Values are presented as mean \pm 1 SD.

Variable	Joint	Slow	Incline
Angle [°]	Hip	10.82 \pm 2.26	9.09 \pm 2.93
	Knee	5.64 \pm 0.87	6.37 \pm 2.59
	Ankle	4.48 \pm 3.21	2.68 \pm 1.36
Moment [Nm/kg]	Hip	0.51 \pm 0.03	0.78 \pm 0.12
	Knee	0.32 \pm 0.08	0.51 \pm 0.13
	Ankle	0.11 \pm 0.02	0.25 \pm 0.06

TRITA-CBH-GRU-2025:048

Stockholm, Sverige 2025

www.kth.se